

Increasing the solar cell power output by coating with transition metal-oxide nanorods

I.A. Kuznetsov^a, M.J. Greenfield^a, Y.U. Mehta^a, W. Merchan-Merchan^b, G. Salkar^a, A.V. Saveliev^{a,*}

^a Department of Mechanical and Aerospace Engineering, North Carolina State University, Raleigh, NC 27695-7910, USA

^b School of Aerospace and Mechanical Engineering, University of Oklahoma, Norman, OK 73019, USA

ARTICLE INFO

Article history:

Received 22 November 2010
Received in revised form 8 April 2011
Accepted 11 April 2011
Available online xxx

Keywords:

Silicon solar cell
Light scattering
Nanoparticles
Transition metal-oxide nanorods

ABSTRACT

Photovoltaic cells produce electric current through interactions among photons from an ambient light source and electrons in the semiconductor layer of the cell. However, much of the light incident on the panel is reflected or absorbed without inducing the photovoltaic effect. Transition metal-oxide nanoparticles, an inexpensive product of a process called flame synthesis, can cause scattering of light. Scattering can redirect photon flux, increasing the fraction of light absorbed in the thin active layer of silicon solar cells. This research aims to demonstrate that the application of transition metal-oxide nanorods to the surface of silicon solar panels can enhance the power output of the panels. Several solar panels were coated with a nanoparticle-methanol suspension, and the power outputs of the panels before and after the treatment were compared. The results demonstrate an increase in power output of up to 5% after the treatment. The presence of metal-oxide nanorods on the surface of the coated solar cells is confirmed by electron microscopy.

© 2011 Elsevier Ltd. All rights reserved.

1. Introduction

The silicon solar cell (SSC) is used to harness solar energy via the photovoltaic effect. The major weakness of SSCs is their low efficiency (5–15% for commercially available cells) due to low utilization of the incident photons by the silicon layer of the cell. There has been an intensive search for methods of enhancing the power output of SSCs. Coating the surface of the cell with nanoparticles has proven to be a promising technique to enhance the efficiency of the cells. Enhancement of optical absorption by SSCs coated with silver nanoparticles was considered in [1–3]. Nishioka et al. [4] investigated the efficiency of antireflective coating of SSCs with gold and silver nanoparticles. Abe and Kajikawa [5] considered optical properties of gold nanoparticles deposited on a metal surface. The maximum current density increase reported in the above references was 8%. Optimization of periodic arrays of metal nanoparticles on the surface of solar cells was studied by Mokkaḩapati et al. [6]. Derkacs et al. [7] investigated the effect of nanoparticle surface concentration on electric power enhancement in solar cells. The enhancement of the efficiency of SSCs is explained by the effect of light scattering that leads to an increase of the optical path of the incident light through the absorbing layer. Theoretical explanation of the effect of nanoparticles is based on analyzing the optical dispersion of light by the nanoparticles (de Waele et al. [8]).

The most readily altered factor in optimizing the utilization of the photovoltaic effect is the thickness of the cells. Scattering theory utilizes the wave properties of light and provides a method of increasing the effective thickness of the panel without using an excessive amount of silicon for each panel. By distributing nanoparticles that can cause scattering across the surface of an SSC, it is possible to redirect the incoming light from a near-perpendicular angle of entry to a near-parallel angle with respect to the surface of the SSC. Thus coating the surface of the solar panels with nanoparticles can make it possible to increase the power output of a SSC.

Relatively little research has been done on application of transition metal-oxide nanoparticles to coat SSC surfaces as a means of increasing their power output. The undertaken research studies whether and to what degree transition metal-oxide nanoparticles can increase the SSC power output. The hypothesis that directed this experimental study states that coating the surface of the SSC with transition metal-oxide nanoparticles will increase the overall power output of the SSCs.

2. Materials and methods

2.1. Nanorod synthesis

Single-step flame synthesis of metal-oxide nanoparticles was performed using transition metal probes inserted into an opposed-flow methane oxy-flame. The high temperature reacting environment of the flame tends to convert the metals into a high

* Corresponding author. Tel.: +1 919 515 5675; fax: +1 919 515 7968.
E-mail address: asaveliev@ncsu.edu (A.V. Saveliev).

density layer of the given transition metal-oxide nanoforms. To identify the most promising metal-oxide nanoform, initial experiments were conducted with several nanomaterials made of Ta₂O₅, WO₃, MoO₃, and NbO₂. Experimental results indicated that of the four nanoparticle coatings, WO₃ nanorods provided the largest increase in power output. Thus, WO₃ nanorods were selected for an in-depth analysis.

Tungsten oxide nanorods were prepared by the flame synthesis method as described elsewhere [9]. The counter-flow flame is similar to the one utilized in our earlier studies on the flame synthesis of carbon [10,11] and molybdenum oxide nanostructures [12]. This counter-flow flame geometry provides a stable one-dimensional reaction front formed by two opposite streams of gases: the fuel (methane seeded with 4% of acetylene) and the oxidizer (50% O₂ + 50% N₂).

The tungsten probe is a 1 mm diameter wire with a purity of 99.9% from Sigma–Aldrich Corporation. The probe is introduced into the essentially 1-D flame radially so that the probe axis is parallel to the reaction front. The residence time of the probe in the flame is close to 2 min. The flame temperature gradients reach ~2000 K/cm, and the chemical environment changes rapidly from a hydrocarbon rich zone on the fuel side of the flame to the oxygen rich zone on the oxidizer side. As a result, the probe position in the flame significantly affects the synthesis processes as reported for carbon and metal-oxide nanomaterials [9–13].

The tungsten oxide nanorods had diameters ranging from 20 to 50 nm and lengths of up to 50 μm. The average length was close to 10 μm. The length could be controlled by the probe residence time. A high density layer of synthesized nanorods was observed to cover the upper probe's surface. This layer was mechanically removed from the probe surface, weighted, and used in coating experiments. No additional purification or filtrations steps were implemented.

2.2. Coating

Three amorphous solar cells (model AM-1815, Sanyo Inc.) were used for the experiments. Each had an effective area of 22.3 cm². The nanorods were diluted in a methanol suspension to facilitate coating of the SSCs. Before the coating, the nanorods suspensions were sonicated to ensure that the nanorods were evenly dispersed in methanol. Subsequently, the suspension was applied to the SSC surface using a volumetric pipette. Early experiments in the spreading of the methanol/nanorod suspension across the surface of the SSC determined that a regular pattern of drops allows the nanoparticles to spread across the surface of the SSC most evenly. This ensured that there would not be large conglomerations of nanoparticles that could alter the results. The coating of one solar panel required about 0.4 mL of nanoparticle suspension. The panels were allowed to dry before testing.

2.3. Power output measurements

The setup consisted of a solid frame that was entirely covered by an ultra-opaque, non-woven black fabric that kept any additional photons from entering or leaving the box (Fig. 1). A fixed halogen light source (model Ace 1, Schott Inc.) with stabilized power output was placed on top of the frame directly above the tested SSC. A radiant spectrum of the selected light source was close to the solar spectrum in a range of spectral sensitivity of the solar cells (0.4–0.8 μm).

The SSCs were placed inside the black box and data was collected every 30 s for 15 min. First, readings for the uncoated SSC were recorded. Readings for the nanorod-coated SSCs were documented next.

Multimeters (model 420, Extech Inc.) were used to record voltage and current. In order to find the actual maximum power, a

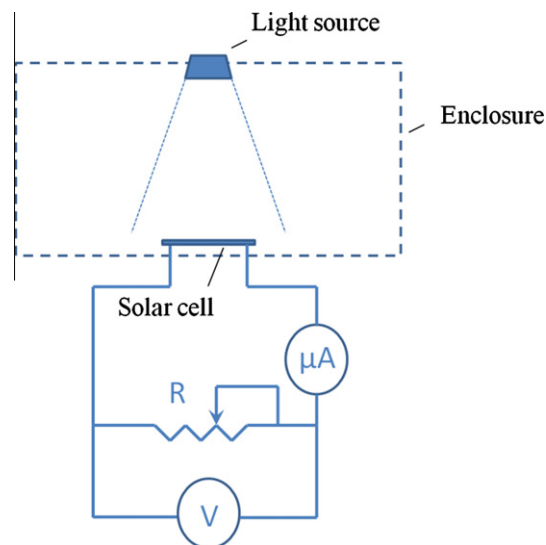


Fig. 1. Schematic of the experimental setup.

voltage–current curve was constructed. This was done by manipulating the resistance of the circuit in order to find current value at various voltages (Fig. 1). The obtained curve was interpolated and the maximum power output was found to be $P = 0.281 V_{OC} I_{SC}$, where I_{SC} and V_{OC} are the short-circuit current and open-circuit voltage of the cell. Subsequently, only the open-circuit voltage and short-circuit current were measured.

3. Results and discussion

Three different concentrations (high, medium, and low) of WO₃ nanorods were tested. A modest increase of power output was observed for the medium concentration of deposited nanorods (Fig. 2). The increase of the output power was attributed to the increase of the short-circuit current. The open-circuit voltage remained practically constant. The short-circuit current from a silicon solar cell is usually nearly proportional to the number of photons absorbed in the photovoltaic layer. This suggests that the light scattering by the deposited nanorod layer improves efficiency of the light absorption.

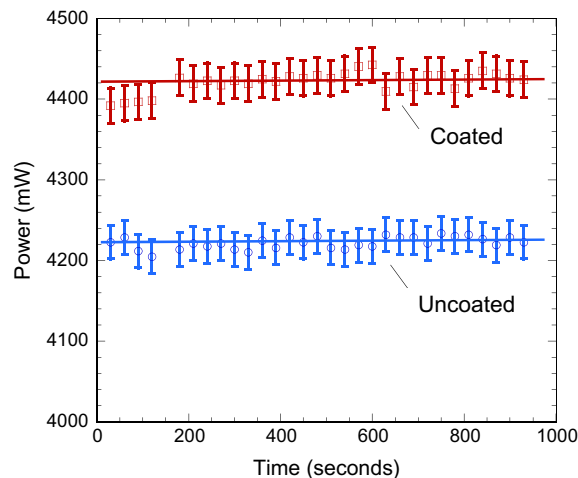


Fig. 2. Power output of uncoated vs. coated solar cell with medium concentration of tungsten oxide/methanol suspension. Bars indicate a 95% confidence interval for measured values.

Table 1 summarizes the result of the data collection providing time-averaged values of short-circuit current \bar{I}_{SC} , open-circuit voltage \bar{V}_{OC} , and power \bar{P} that was calculated as $\bar{P} = 0.281 \cdot \bar{I}_{SC} \bar{V}_{OC}$

In order to establish statistical significance of these data, results were analyzed using Student's *t*-test [14], a statistical hypothesis test in which the test-statistic is based upon a *t*-distribution. This test provides an accurate test-statistic because it is not particularly sensitive to outliers in data. The robust nature of this distribution allows for assumed normality given a relatively large sample size (usually defined as 30 or more samples). The collected data satisfies this requirement, and as a result normality could be assumed. Due to the nature of the collected information, the high concentration data was analyzed using a two-sample *t*-test, while the low and medium concentration data was analyzed using a paired *t*-test. The null hypothesis tested was that power output of the uncoated panel equals the power output of the coated panel, while the alternate hypothesis was that power output of the uncoated panel is less than the power output of a coated panel. Results of the *t*-test are documented in Table 2; the alternate hypothesis is clearly favored.

To further ensure that the power increase described in the above results is indeed caused by the nanoparticle coating, electron microscopy was utilized in order to analyze the surface of the SSC. Fig. 3a and b displays scanning electron microscope images of the SSC surface after coating with high and medium concentrations of tungsten oxide/methanol suspension. Energy-dispersive X-ray spectroscopy conducted on the surface of the solar panel indicated the presence of WO_3 on the surface.

Analysis of data collected provides favorable results. Measured values show an increase in power output of SSCs after coating with all tested concentrations of tungsten oxide nanoparticles. The results clearly support the hypothesis: gathered data shows a defi-

Table 1
Average voltage, current and power output recorded before and after the coating.

Before coating			Concentration	After coating			$\Delta\bar{P}$ (%)
\bar{V}_{OC} (V)	\bar{I}_{SC} (μ A)	\bar{P} (μ W)		\bar{V}_{OC} (V)	\bar{I}_{SC} (μ A)	\bar{P} (μ W)	
6.35	2757	4925	High (0.1 mg/mL)	6.35	2770	4947	+0.5
6.48	2316	4222	Medium (0.01 mg/mL)	6.49	2421	4422	+5
6.35	2734	4883	Low (0.001 mg/mL)	6.34	2771	4939	+1.15

Table 2
Results of statistical analysis.

Concentration	Test	<i>t</i> -value	<i>p</i> -value	Statistically significant increase?
High	Two Sample <i>t</i> -test	3.4	0.0016	Yes
Medium	Paired <i>t</i> -test	78.7	1.1E-35	Yes
Low	Paired <i>t</i> -test	12.9	7.3E-14	Yes

nite trend toward an increase in power after coating the SSCs. For all concentrations used, the current increase was the primary cause of the power increase. This is not unexpected because the electromotive force produced is generally invariant.

The low concentration coating had a positive effect of 1.15% on the power output. This supports the proposed hypothesis, but the relatively low increase is attributed to the fact that the concentration was most likely too low to appreciably increase the amount of light absorbed by the panel. Coating with the diluted nanoparticles suspension did cause the desired power increase, but only to a small degree because of the low concentration of the deposited nanoparticles on the surface of the SSC.

At the highest concentration, the positive effect on the power output was even smaller suggesting that the large amounts of tungsten oxide nanorods on the surface completely covered the surface of the SSC and partially blocked the light from striking the surface of the solar cell (see Fig. 3a).

On the other hand, the medium concentration suspension of tungsten oxide nanoparticles maximized the desired scattering effect among the tested concentrations, showing an increase in power output of 5% after coating. Fig. 2 summarizes the SSC power output vs. time measured for this case. Note the large difference between coated and uncoated SSC power output values, with the 95% confidence intervals of measured power output values being a considerable distance apart. The medium concentration coating (see Fig. 3b) thus ensured that both not many agglomerates of nanoparticles would form and that there would be sufficient nanoparticles on the surface to induce the scattering effect.

The slight variability in actual power output values collected can be attributed to two factors. First, there is always random variation in experimental data, in this case because of the accuracy of the multimeter used (accuracy of $\pm 0.5\%$). Second, the temperature of the apparatus may have varied by several degrees over the trials. The slight differences in temperature over time have an effect on the internal resistance of the SSC. Since silicon is a semiconductor, its resistance decreases with increasing temperature. Further study

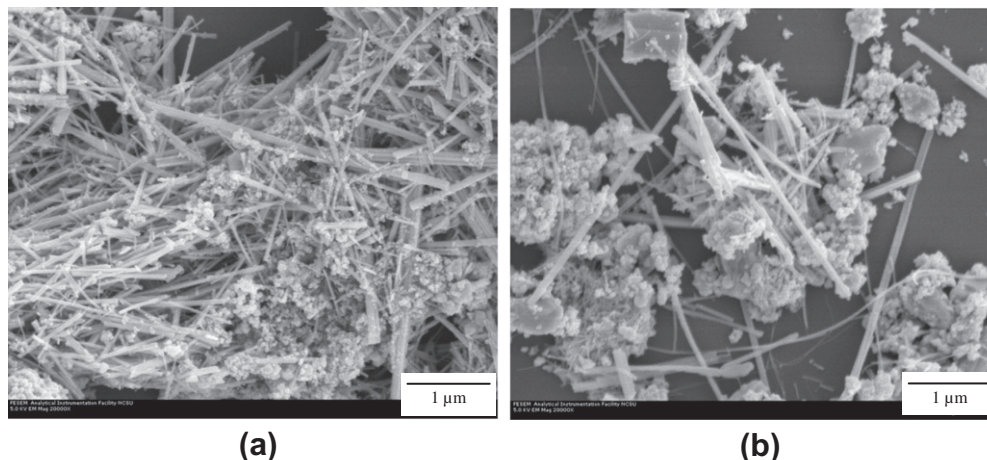


Fig. 3. Scanning electron microscope images of tungsten oxide nanorods on the surface of the silicon solar cell: (a) high concentration, and (b) medium concentration.

is required to ascertain the effect of temperature on the efficiency of nanoparticle-coated SSCs.

It can be estimated that the prepared coatings correspond to the nanorod densities of 1–100 nanorods per square micron. Irregular multilayer deposits of nanorods are expected at high concentrations. This is confirmed by the image shown in Fig. 3a. In this case non-aligned nanorods pile up forming an irregular coating with a 3-D structured layer. The layer has a characteristic thickness of a few microns. Light transfer in this dense nanorod layer is quite complex and some losses are expected. In addition, the coating prepared from the suspension with the high nanorod concentration cover the solar cell surface in a non-homogenous manner living bare spots on the surface (Fig. 3a). At the medium coating density (Fig. 3b) the nanorods in the coating are mostly parallel to the surface. In this case the coating thickness is approximately a few nanorod diameters. The layer is clearly transparent to the light. Amorphous impurities present in the solution affect the coating structure and reduce its efficiency. Further optimization of the coating can be achieved by using purified nanorod suspensions and modifying coating methods. For example, spin-coating and electro-spray techniques could be applied to improve coating uniformity and to create aligned nanorod layers. Effects related to nanorods morphology and structure, such as crystallinity, length, diameter, and length-to-diameter ratio, are important and merit further studies. Finally, the stability and durability of the coating have to be addressed.

4. Conclusions

Analysis of power output between pristine SSCs and SSCs coated with all three concentrations of tungsten oxide nanoparticles showed statistically significant increases in power output of up to 5% after coating. The absence of other factors that could induce an increase in power output of the SSC after coating indicates that the nanoparticles did indeed cause the power output to increase. The experiments demonstrated that the transition metal-oxide nanoparticles are an effective replacement for gold, silver, and titanium nanoparticles, which have already been shown to increase SSC power generation.

Acknowledgements

The support of the work on nanomaterial synthesis and characterization by the National Science Foundation through the Collaborative Research Grants CTS-0854433 and CTS-0854006 is gratefully acknowledged.

References

- [1] Moulin E, Sukmanowski J, Schulte M, Gordijn A, Royer FX, Stiebig H. Thin-film silicon solar cells with integrated silver nanoparticles. *Thin Solid Films* 2008;516:6813–7.
- [2] Luo PQ, Moulin E, Sukmanowski J, Royer FX, Dou XM, Stiebi H. Enhanced infrared response of ultra thin amorphous silicon photosensitive devices with Ag nanoparticles. *Thin Solid Films* 2009;517:6256–9.
- [3] Nakayama K, Tanabe K, Atwater HA. Plasmonic nanoparticle enhanced light absorption in GaAs solar cells. *Appl Phys Lett* 2008;93:121904.
- [4] Nishioka K, Horita S, Ohdaira K, Matsumura H. Antireflection subwavelength structure of silicon surface formed by wet process using catalysis of single nano-sized gold particle. *Sol Energy Mater Sol Cells* 2008;92:919–22.
- [5] Abe S, Kajikawa K. Linear and nonlinear optical properties of gold nanospheres immobilized on a metallic surface. *Phys Rev B* 2006;74:035416.
- [6] Mokkaapati S, Beck FJ, Polman A, Catchpole KR. Designing periodic arrays of metal nanoparticles for light-trapping applications in solar cells. *Appl Phys Lett* 2009;95:053115.
- [7] Derkacs D, Lim SH, Matheu P, Mar W, Yu ET. Improved performance of amorphous silicon solar cells via scattering from surface plasmon polaritons in nearby metallic nanoparticles. *Appl Phys Lett* 2006;89:093103.
- [8] de Waele R, Burgos SP, Polman A, Atwater HA. Plasmon dispersion in coaxial waveguides from single-cavity optical transmission measurements. *Nano Lett* 2009;9:2832–7.
- [9] Merchan-Merchan W, Saveliev AV, Jimenez WC, Salkar G. Flame synthesis of hybrid nanowires with carbon shells and tungsten-oxide cores. *Carbon* 2010;48:4510–8.
- [10] Saveliev A, Merchan-Merchan W, Kennedy LA. Metal catalyzed synthesis of carbon nanostructures in an opposed flow methane oxygen flame. *Combust Flame* 2003;135:27–33.
- [11] Merchan-Merchan W, Saveliev AV, Kennedy LA. High-rate flame synthesis of vertically aligned carbon nanotubes using electric field control. *Carbon* 2004;42:599–608.
- [12] Merchan-Merchan W, Saveliev AV, Kennedy LA. Flame synthesis of molybdenum oxide whiskers. *Chem Phys Lett* 2006;422:72–7.
- [13] Li TX, Kuwana K, Saito K, Lu C, Chen Z. Influences of temperature and available carbon sources on synthesis of carbon nanotubes in methane-air diffusion flames. *Proc Combust Inst* 2009;32:1855–61.
- [14] Snedecor GW, Cochran WG. *Statistical methods*. 8th ed. Iowa State University Press: Ames; 1989.